

# Effects of Injection Conditions on Flame Structures in Gas-Centered Swirl Coaxial Injector

Wooseok Song, Sunjung Park, Jongkwon Lee, Jaye Koo

**Abstract**—The objective of this paper is to observe the effects of injection conditions on flame structures in gas-centered swirl coaxial injector. Gaseous oxygen and liquid kerosene were used as propellants. For different injection conditions, two types of injector, which only differ in the diameter of the tangential inlet, were used in this study. In addition, oxidizer injection pressure was varied to control the combustion chamber pressure in different types of injector. In order to analyze the combustion instability intensity, the dynamic pressure was measured in both the combustion chamber and propellants lines. With the increase in differential pressure between the propellant injection pressure and the combustion chamber pressure, the combustion instability intensity increased. In addition, the flame structure was recorded using a high-speed camera to detect CH\* chemiluminescence intensity. With the change in the injection conditions in the gas-centered swirl coaxial injector, the flame structure changed.

**Keywords**—Liquid rocket engine, flame structure, combustion instability, dynamic pressure.

## I. INTRODUCTION

THE high efficiency and high performance of the liquid rocket engine is essential in the development of space launch vehicles. For liquid propellant rocket applications, the staged combustion cycle has been used to improve the efficiency and performance of the liquid rocket engine [1], [2]. The staged combustion cycle requires an injector for the gas-liquid propellant, and relevant research has been conducted for several years. However, the research of the gas-centered swirl coaxial injector has not been clearly understood because of its complex design as evidenced by the calculation of dynamic characteristics. The gas-centered swirl coaxial injector is an airblast atomizer; the central gas jet that breaks up the liquid sheet into drops is a key factor to determine the quality of the atomization. Therefore, the objective of this study is to observe the effects of altering injection conditions on the flame structure using the gas-centered swirl coaxial injector. For injection conditions, the mass flow rate and differential pressure between the combustion chamber pressure and the injection pressure are varied to control the momentum flux ratio. A high-speed camera is positioned to capture the flame structure that is visualized from the CH\* chemiluminescence in the hot fire test.

W. Song, S. Park, and J. Lee are with Graduate School of Korea Aerospace University, Goyang, 10540 Korea, Republic of (e-mail: pramodel@kau.kr, tjswd9986@kau.kr, leejk1120@kau.kr).

J. Koo is with Korea Aerospace University, Goyang, 10540 Korea, Republic of (e-mail: jykoo@kau.ac.kr).

## II. EXPERIMENTAL SETUP

### A. Experimental Facility

A gas-centered swirl injector was used to inject the propellant in this study. Fig. 1 shows the schematic of propellant supply lines. Fig. 2 represents the schematic of the injector. Two types of injectors were used to obtain different injection conditions. The only difference is the diameter of the tangential inlet ( $d_m$ ). The experimental cases are listed in Table 1. The diameter of the tangential inlet in Case I is 0.5 mm and in Cases II to V, it is 0.2 mm. The diameter of the oxidizer injector ( $d_g$ ) is 8.0 mm, and the inner ( $d_i$ ) and outer diameter ( $d_o$ ) of the fuel injector are 10.0 mm and 12.0 mm, respectively. The recess length  $R$ , which improves the performance of breakup and atomization, was designed to be 10.0 mm. In addition, the width ( $L_w$ ), height ( $L_h$ ), and length ( $L_c$ ) of the combustion chamber are 66 mm, 50 mm, and 188 mm, respectively. In order to visualize the flame, quartz was installed in the combustion chamber wall. A spark plug (NGK CR9EIX), which supplies ignition energy of 90 mJ, was used. The sparking rate was 48 Hz, and the spark duration was 125 ms.

A propellant and a data acquisition system were developed for the hot firing test, as shown in Fig. 2. High pressure gaseous nitrogen was used to pressurize the liquid fuel in the tank. The gaseous oxygen for the oxidizer was injected directly from the oxidizer tank, and the flow rate was controlled by the choking orifice. In order to prevent flame backfire from the combustion chamber to the propellant lines, check valves were installed in the supply lines. The volumetric flow rates were measured using a turbine flow meter, and the mass flow rates of the propellant were calculated from the volumetric flow rate and density, which in turn were estimated from the temperature and pressure.

### B. Combustion Instability Intensity

In the combustion region, chemiluminescence refers to the phenomenon of spontaneous photon emission, i.e. light, including ultraviolet and infrared rays [3]. The representative species related to the combustion process are OH\*, CH\*, and C<sub>2</sub>\*. CH chemiluminescence intensity was measured to confirm the flame structures under different injection conditions. Its images were recorded using a high-speed camera with a 430-nm band pass filter. The camera was set with an acquisition rate of 1000 fps and a shutter speed of 1/1000 s. The resolution was 1024 x 1024 pixels.

The combustion instability intensity was calculated using (1) to compare combustion instability between cases as listed in Table I [4], [5].

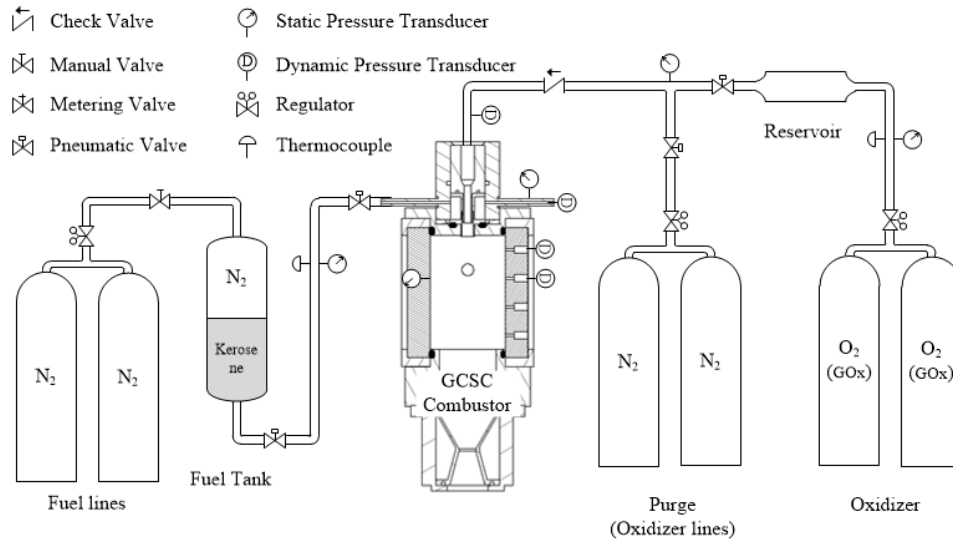


Fig. 1 Schematic of propellant supply lines

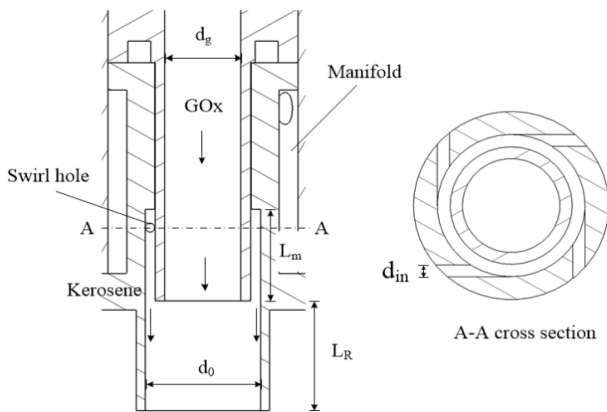


Fig. 2 Schematic of gas-centered swirl injector

$$F = P'_{rms} / P_c \times 100 \quad (1)$$

where  $P'_{rms}$  is the fluctuation pressure measured using the dynamic pressure transducer, and  $P_c$  is the averaged chamber pressure.

TABLE I  
EXPERIMENTAL CONDITIONS

	Case I	Case II	Case III	Case IV	Case V
$d_{in} (mm)$	0.5		0.2		
$P_{cc} (MPa)$	0.92	0.71	0.85	0.91	0.98
$P_{inj-f} (MPa)$	1.21	1.38	1.40	1.38	1.39
$P_{inj-ox} (MPa)$	1.07	0.94	1.17	1.29	1.47
$O/F$	1.66	2.04	2.85	3.28	3.79
Momentumflux ratio	19.41	18.91	30.91	39.18	48.59

### C. Experimental Conditions

The experiments in this study were performed to ascertain the effects of injection conditions on flame structures using a gas-centered swirl injector. An analysis was performed to compare the data under different injection conditions. Table I

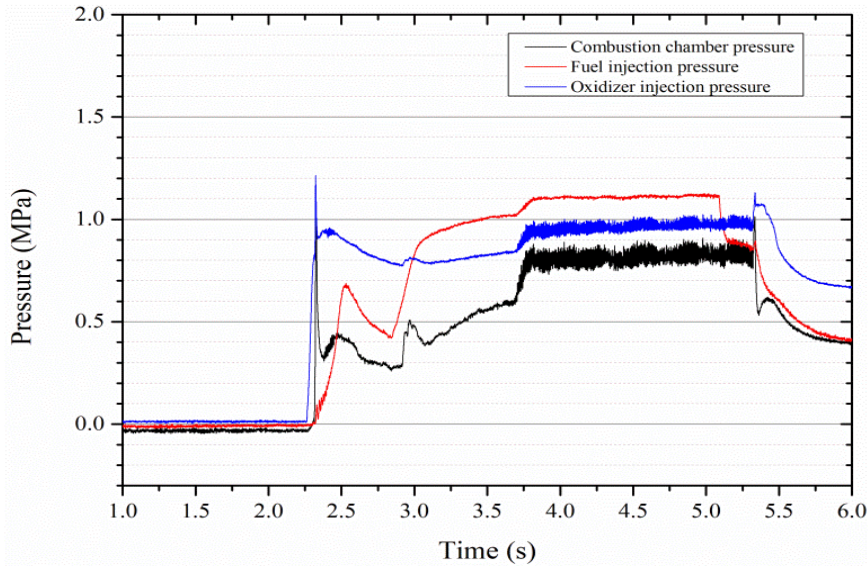
lists the experimental results. The combustion chamber pressure was approximately 0.9 MPa, and the fuel injection pressure was approximately 1.3 MPa. The oxygen injection pressure, however, was varied to apply different injection conditions and similar combustion chamber pressure for each case.

## III. RESULTS AND DISCUSSION

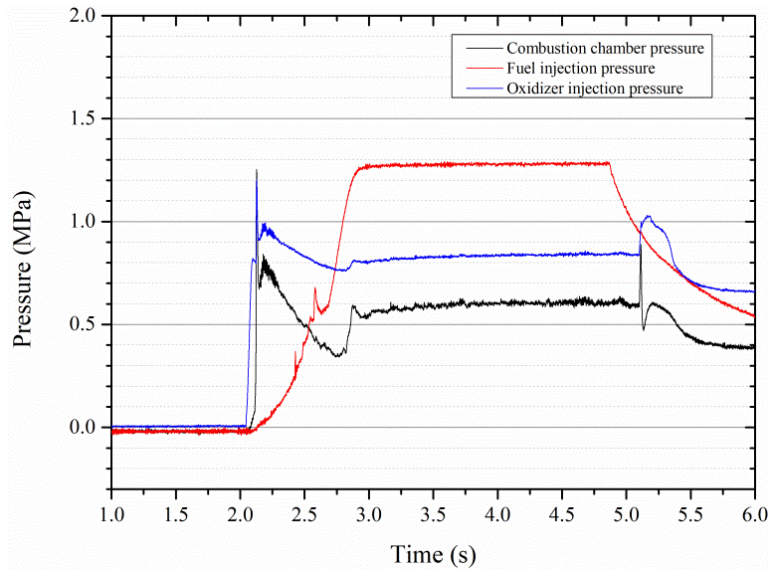
### A. Effect of Injection Condition on Combustion Instability

Fig. 3 represents the combustion chamber ( $P_{cc}$ ) and injected propellant pressure in Cases I and II. The overall runtime of the hot firing test was 3 s, which was enough to detect the steady-state condition. As shown in Fig. 3 there is a flame development period after initial ignition. The supply pressure condition between Cases I and II was the same, but the diameter of the tangential inlet was different. This caused a change of differential pressure between the injection propellant pressure and combustion chamber pressure. During the steady-state condition, the combustion chamber pressure in Case I was more unstable than that in Case II, which is confirmed by the data of the dynamic pressure transducer as shown in Fig. 4. The data analysis interval was 0.1 s and 0.25 s, respectively. The wave shape was similar as a result of the similar frequency. This is because the high differential pressure between propellant injection pressure and combustion chamber pressure allows the propellant to inject smoothly; hence the combustion chamber pressure was stable in the Case II.

The Fast Fourier Transform was performed to observe the difference of frequency amplitude from the data of the dynamic pressure as shown in Fig. 5. The dominant frequency was approximately 153 Hz. The amplitude of Case I was higher than that of Case II. This was expected because the combustion chamber pressure in Case I had more fluctuation than that in Case II.

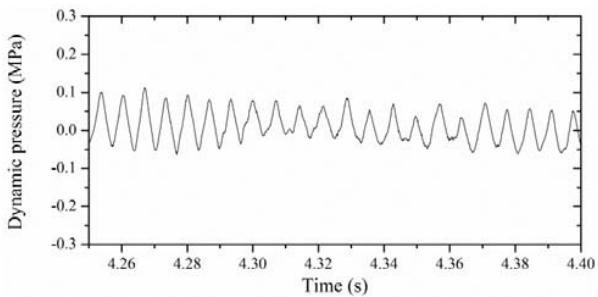


(a)

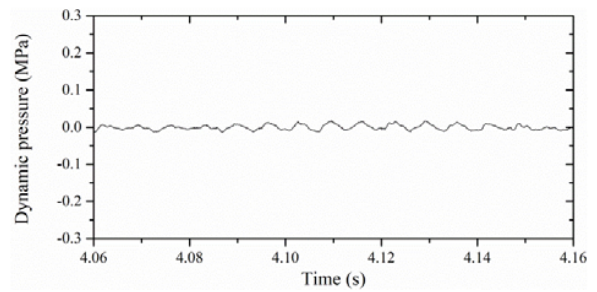


(b)

Fig. 3 Combustion chamber pressure (a) Case I, and (b) Case II



(a)



(b)

Fig. 4 Dynamic pressure (a) Case I, and (b) Case II

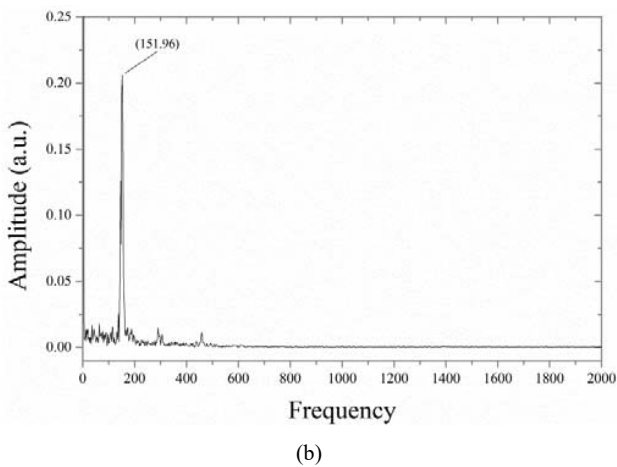
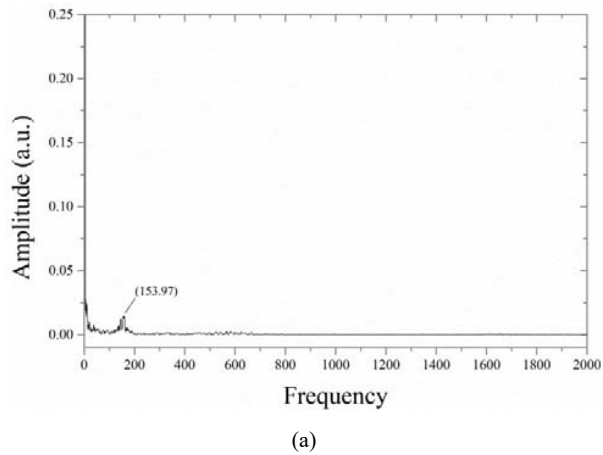


Fig. 5 Spectra of dynamic pressure (a) Case I, and (b) Case II

#### B. CH\* Chemiluminescence Images

In order to observe the combustion instability with respect to the injection conditions, the combustion instability intensity was calculated from (1). Calculated values of the combustion instability intensity are shown in Fig. 6. The value of 10% from (1) could be referred to determine the combustion instability. In Cases II to V, the combustion instability intensity increases with an increase in the injection pressure of the oxidizer. From this result, it was confirmed that combustion instability intensity is affected by the injected oxidizer: the unstable oxidizer injection influenced the flame. In order to confirm the flame structures, CH\* chemiluminescence images were recorded using a high-speed camera. Fig. 7 shows visualized CH\* chemiluminescence images in Cases I to II. These images represent the averaged images during the steady-state condition. The spray angle of the injected propellant was calculated using images. In all cases, the spray angle was calculated to be small. This is because the jet stream of the gaseous oxidizer is dominant in the breakup and atomization process. Although the spray angle was small, there were slight differences under different injection conditions. The spray angle in Case I was calculated to be 5.93 degrees, and in Case II it was calculated to be 9.54 degrees.

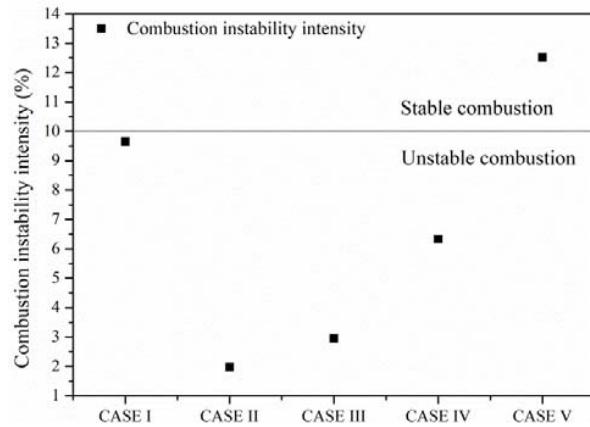


Fig. 6 Combustion instability intensity with respect to injection conditions

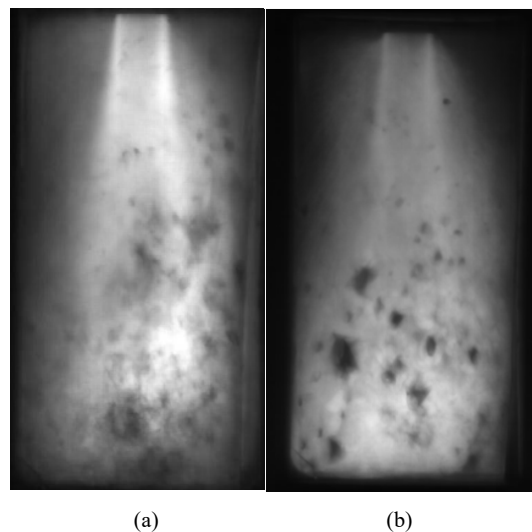


Fig. 7 CH\* chemiluminescence images (a) Case I, and (b) Case II

The reason for this difference is that the swirl intensity increased with the increase in the differential pressure between the propellant injection pressure and the combustion chamber pressure.

#### IV. CONCLUSIONS

In this study, an experiment was designed to observe the effects of propellant injection conditions on the flame structure. A stable combustion is important in terms of the safety of liquid-fueled rocket systems. The combustion instability intensity was calculated from the data of the dynamic pressure transducer, which allows fluctuation of the amplitude of pressure in the combustion chamber. The result was confirmed that the combustion instability intensity increased with an increase in the differential pressure between the propellant injection pressure and the combustion chamber pressure. In addition, the combustion instability intensity was calculated to be higher in high swirl intensity than in low swirl intensity. These phenomena were confirmed with the visualized CH\*

chemiluminescence images. The result from the images was that the spray angle increased with the increase in the differential pressure.

#### ACKNOWLEDGMENT

This work was supported by a National Research Foundation of Korea (NRF) grant funded by the Korean Government (MISP) (NRF-2017M1A3A3A02015233).

#### REFERENCES

- [1] G. P. Sutton, "History of liquid-propellant rocket engines in the United States," *J. Propuls. Power*, vol. 19 pp. 978-1007, Nov. 2003.
- [2] D. R. Ballal, and A. H. Lefebvre, "Ignition of liquid fuel sprays at subatmospheric pressures," *Comb. Flame*, vol. 31, pp. 115-126, 1978.
- [3] T. Lieuwen, H. Torres, and B. T. Zinn, "A mechanism of combustion instability in lean premixed gas turbine combustors," *J. Eng. Gas Turbines Power*, vol. 123, pp. 182-189, 2000.
- [4] R. S. Fry, and M. D. Klem, "Guidelines for combustion stability specifications and verification procedures for liquid propellant rocket engines," CPLA Publication, 655.
- [5] S. Wooseok, K. Dohun, L. Keonwoong, S. Bongchul, K. Sangho, and K. Jaye, "Effects of kerosene heating on dynamic characteristics of GOx/kerosene combustor," *Acta Astronaut*, vol. 126, pp. 528-535, 2016.